Supplementary Figure S1

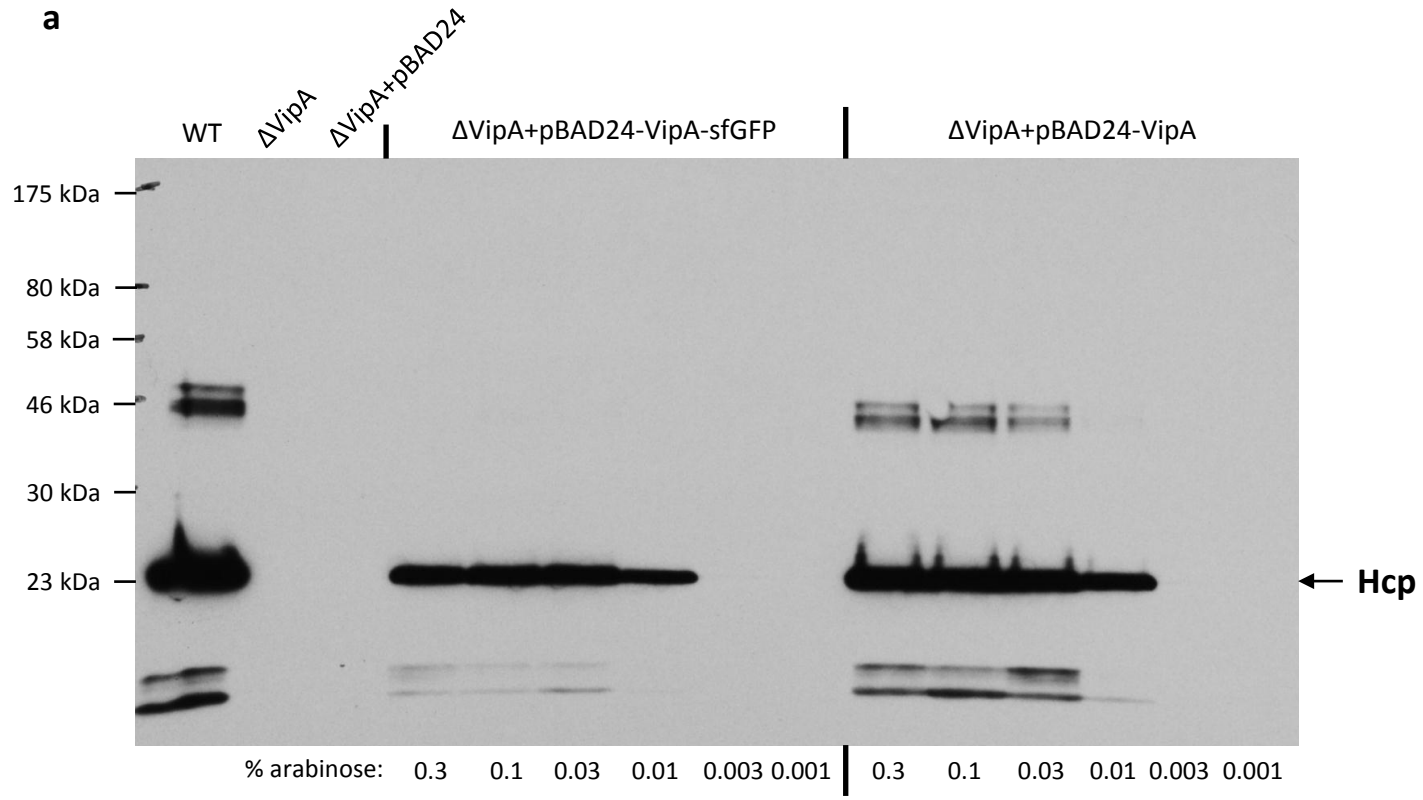

Supplementary Figure S1

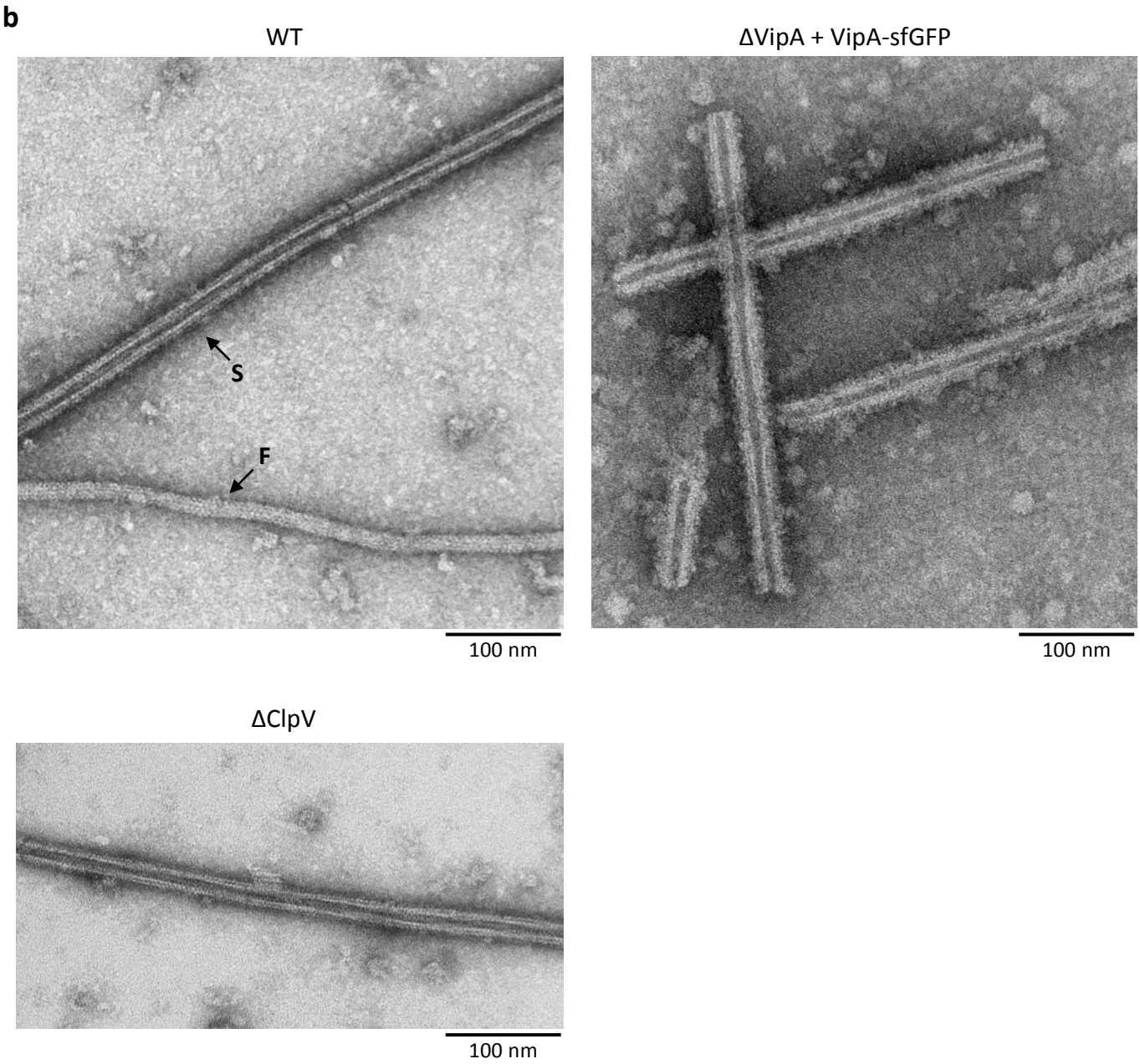

Supplementary Figure S1. VipA-sfGFP complementation. (a) Hcp secretion. *V. cholerae* 2740-80 WT and ΔVipA carrying indicated plasmids were cultivated in the presence of the indicated levels of arabinose. Protein samples were prepared as described in Methods. Hcp protein was detected in cell free supernatant by western blot using anti-Hcp peptide specific antibody. **(b) Sheath structure.** Sheath was isolated from cytosol of *V. cholerae* 2740-80 WT (on the top left), ΔVipA complemented by pBAD24-VipA-sfGFP induced by 0.03% arabinose (on the top right), or ΔClpV (bottom left) by ultracentrifugation. Sheath structure was visualized by negative stain EM. F – flagellum, S – sheath.

Supplementary Figure S2

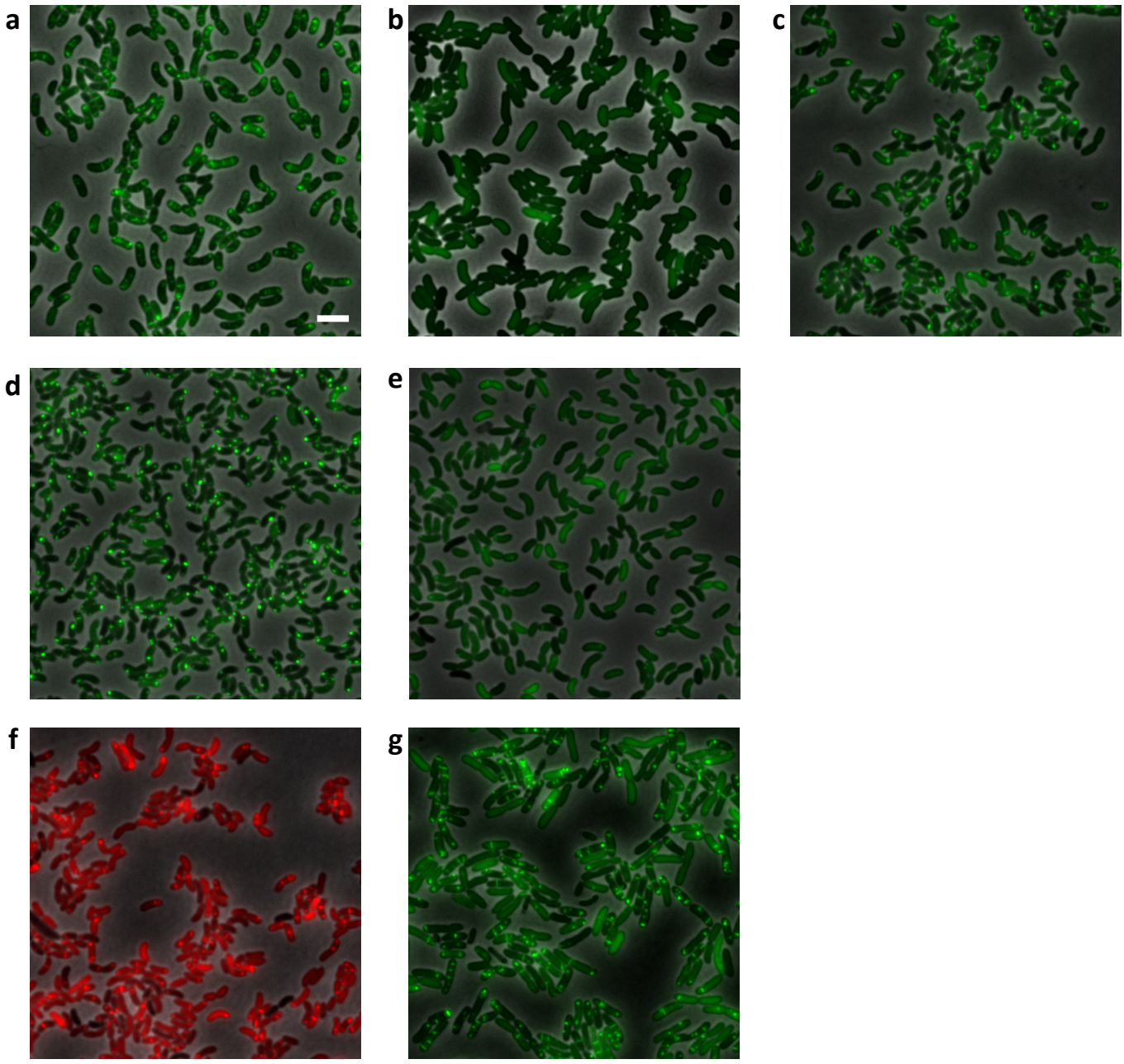

Supplementary Figure S2. Fluorescence microscopy of VipA fluorescent protein fusions. All strains were cultivated under same conditions described in Methods. 30x30 µm field of cells is shown. Bar is 3 µm. **(a)** *V. cholerae* 2740-80 + pBAD24-VipA-sfGFP – VipA-sfGFP in wild-type cells assembles into straight and thin structures of various lengths (up to 5 per cell). **(b)** 2740-80 ΔVipB – in ΔVipB background VipA-sfGFP is diffusely distributed in the cytosol. **(c)** 2740-80 ΔVipA + pBAD24-VipA-sfGFP – both long and short VipA-sfGFP structures are detectable in the cells (additional frames in **Supplementary Video 2**), **(d)** 2740-80 ΔVipA/ΔClpV + pBAD24-VipA-sfGFP – only short VipA-sfGFP structures are detectable in the cells (**Supplementary Video 8**), **(e)** 2740-80 ΔVipA/ΔVCA0109 + pBAD24-VipA-sfGFP – VipA-sfGFP is diffusely distributed in the cytosol with only rare structures detectable (**Supplementary Video 9**), **(f)** 2740-80 ΔVipA + pBAD24-VipA-mCherry2 – VipA-mCherry2 forms structures similar to VipA-sfGFP (**Supplementary Video 7**), **(g)** V52 ΔVipA + pBAD24-VipA-sfGFP – similar VipA-sfGFP structures as in 2740-80 strain are visible in the cells (**Supplementary Video 6**).

Supplementary Figure S3

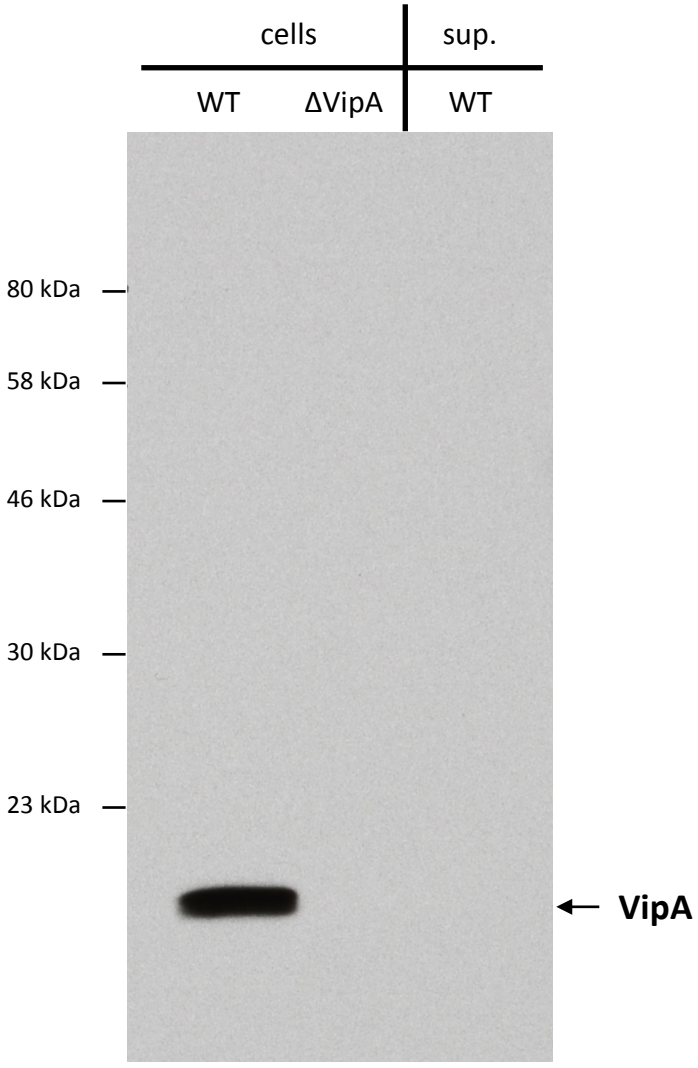

Supplementary Figure S3. VipA localization. Protein samples from wild type *V. cholerae* strain 2740-80 (WT) or derivative carrying a *vipA* in-frame deletion were prepared as described in Methods. VipA protein was detected in cells or cell free supernatant (sup.) by western blot using anti-VipA peptide specific antibody. Absence of the signal in ΔVipA cells confirms specificity of the antibody. VipA protein was detected only in cellular fraction (cells) of WT 2740-80 strain but was undetectable in cell free supernatant (sup.).

Supplementary Figure S4

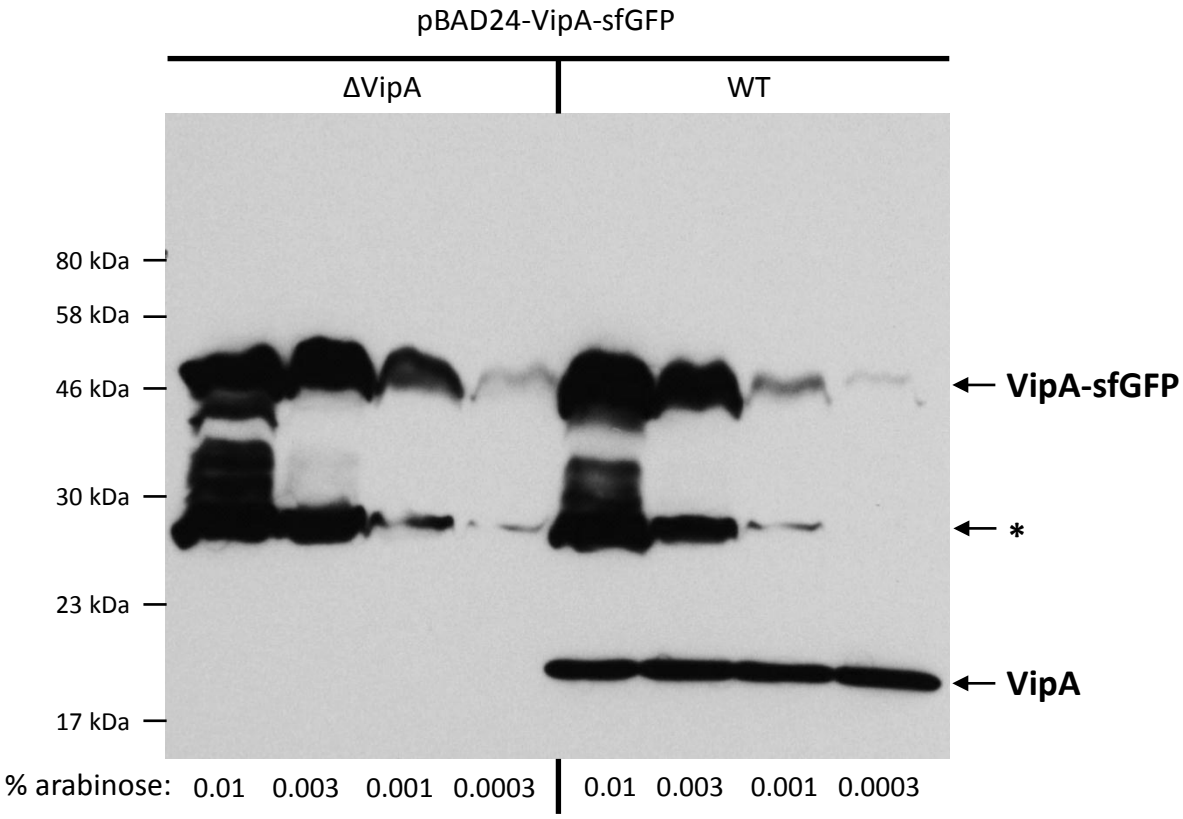

Supplementary Figure S4. **VipA-sfGFP expression level, protein stability.** Wild type *V. cholerae* strain 2740-80 (WT) or a derivative carrying a *vipA* in-frame deletion (both carrying plasmid pBAD24-VipA-sfGFP) were cultivated in the presence of the indicated levels of arabinose. VipA and VipA-sfGFP proteins were detected in cells by western blot using anti-VipA peptide specific antibody. The full length VipA-sfGFP fusion protein migrates at approximately 46 kDa, and WT VipA at 19 kDa. The asterisk indicates bands corresponding to breakdown fragments of VipA-sfGFP that retain VipA epitopes.

Supplementary Figure S5

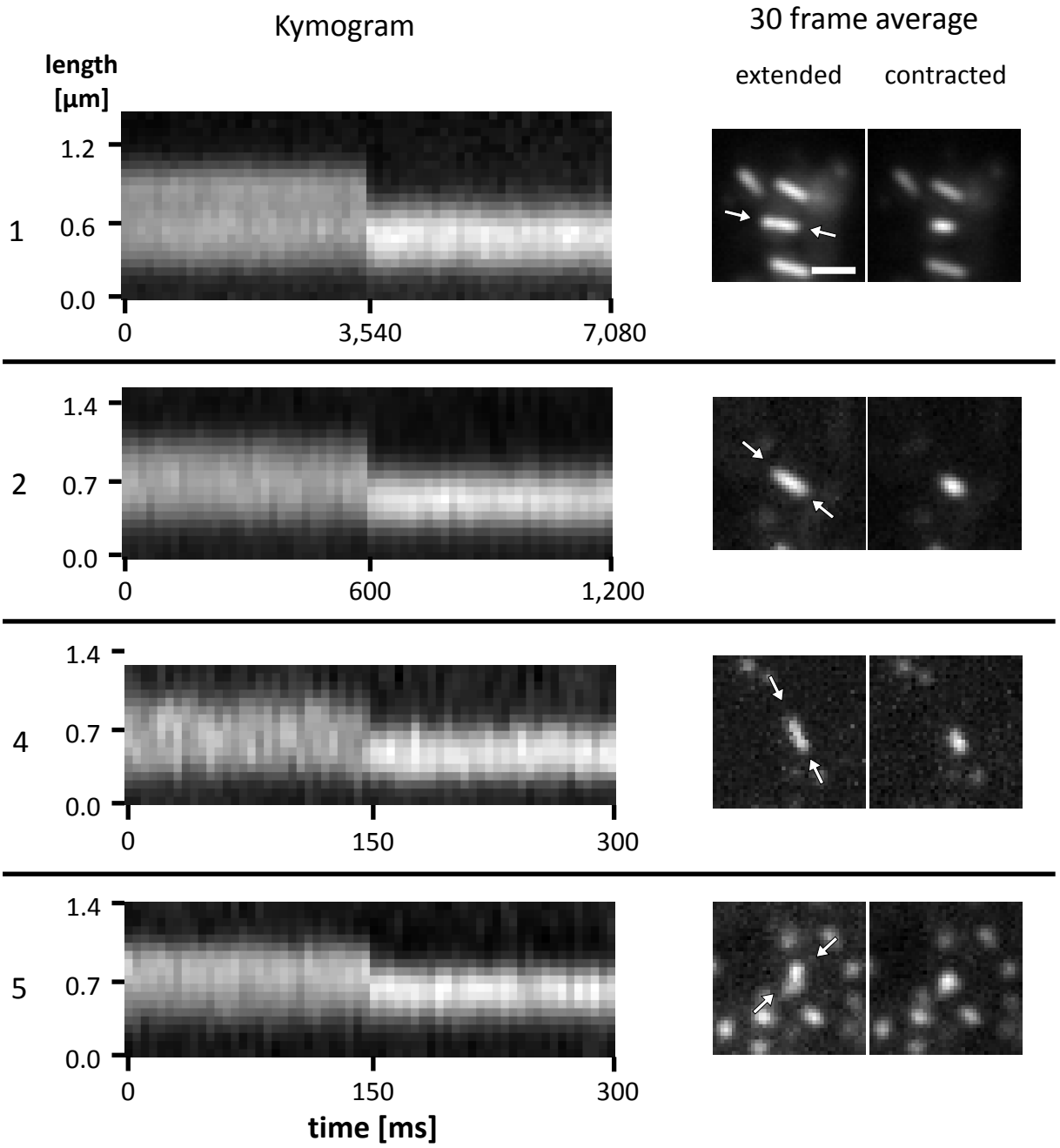

Supplementary Figure S5. High speed imaging of sheath contraction. Kymograms on the left are illustrating rapid change in the length of VipA-sfGFP structure. Projection of signal intensity in time along the axis of the maximal intensity on an extended structure (30 frame average shown on the right) showing a contraction in length and increase in maximal intensity of the contracted structure (30 frame average shown on the right). Arrows indicate contracting VipA-sfGFP structure and mark start and end of a line for generating the kymogram. Gaussian blur filter (sigma radius = 1) was applied to individual frames prior to generating the kymogram for events number 2, 4 and 5. Event 1 was analyzed at speed of 8.5 frames per second (50 ms exposure), event 2 at 50 frames per second (20 ms exposure), and event 4 and 5 at 200 frames per second (5 ms exposure). Bar shown on the first average frame is 1 µm long. All 60 frames of the time-lapse sequence are shown in **Supplementary Video 3** (corresponding numbers of the video segments are shown on the left) together with the contraction event shown in **Figure 1b** (video segment number 3).

Supplementary Figure S6

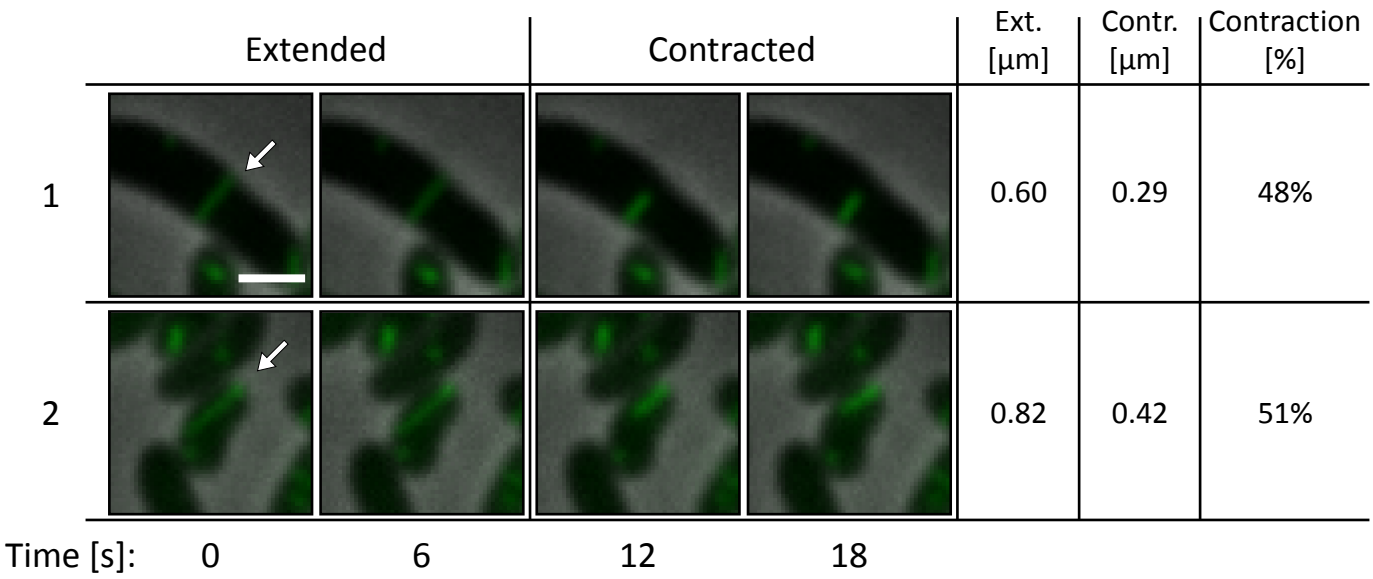

Supplementary Figure S6. Measurement of contraction. Culture of *V. cholerae* 2740-80 ΔVipA strain carrying plasmid pBAD24-VipA-sfGFP was induced by arabinose and imaged as described in Methods. Individual 3x3 µm frames from a time-lapse imaging with a frame rate of 6 sec per frame are shown. 2 frames of sheath in an extended conformation and 2 frames of sheath in a contracted conformation are shown to illustrate the change in length. Bar shown on the first frame of the first time-lapse is 1 µm long. The length of an extended and a contracted sheath was estimated by analysis of an intensity of the fluorescence signal alone.

Supplementary Figure S7

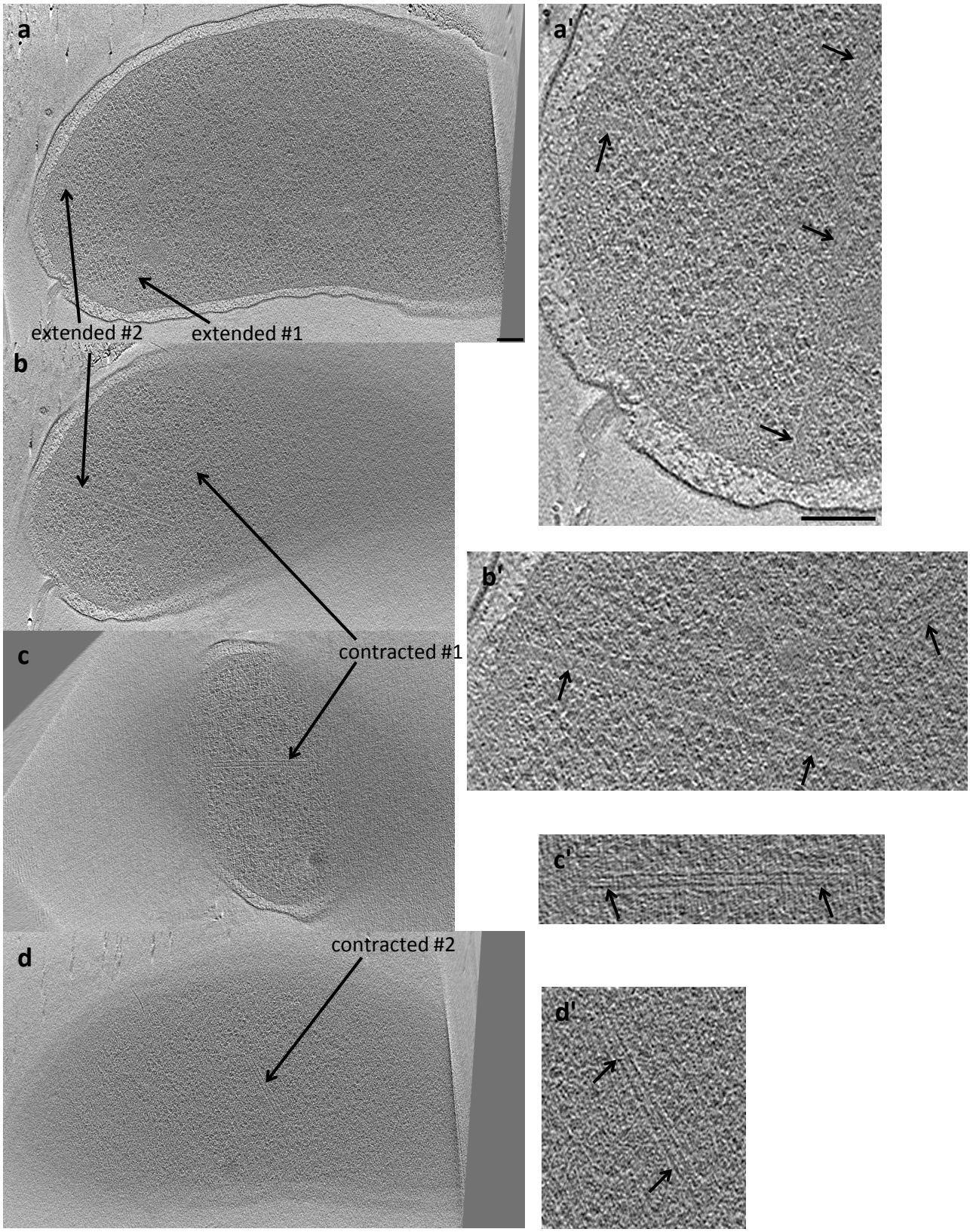

Supplementary Figure S7. **Cell with multiple T6SS sheaths visible.** Various cryotomographic slices (19-nm thick) through the 3-D reconstruction of a single wild-type cell are shown along planes where T6SS structures are present. Two extended and two contracted structures can be seen (arrows). Bars 100 nm. Bar in (a) applies to (a-d), bar in (a') applies to (a'-d').

Supplementary Figure S8

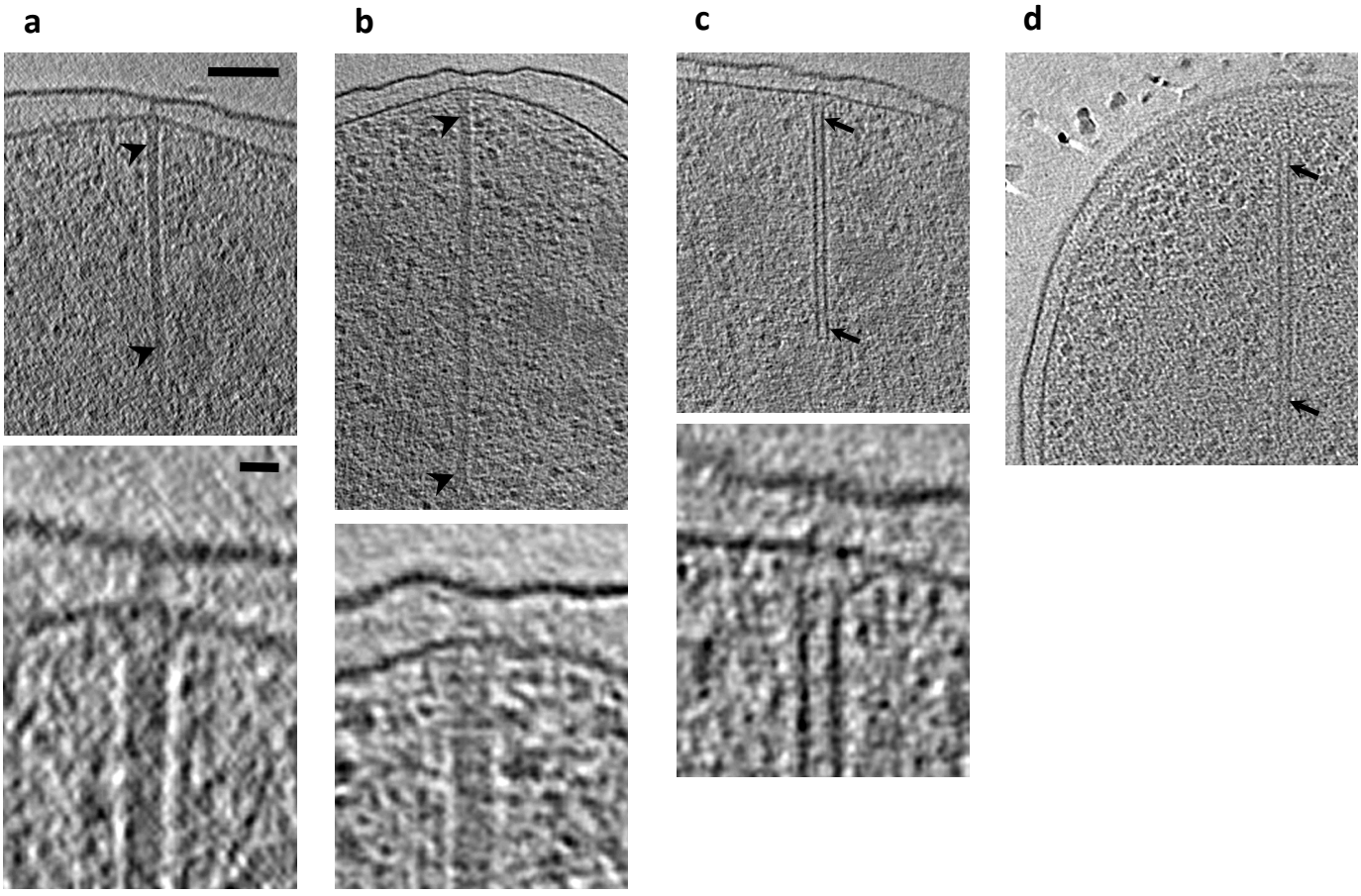

Supplementary Figure S8. **Additional examples of T6SS structures.** Extended (a, b, arrowheads) and contracted (c, d, arrows) T6SS structures found in wild type cells. The baseplate/spike regions are shown enlarged (lower panels in a-c). The slices shown are 19-nm thick. Scale bars 100 nm in overviews, 10 nm in enlarged views.

Supplementary Figure S9

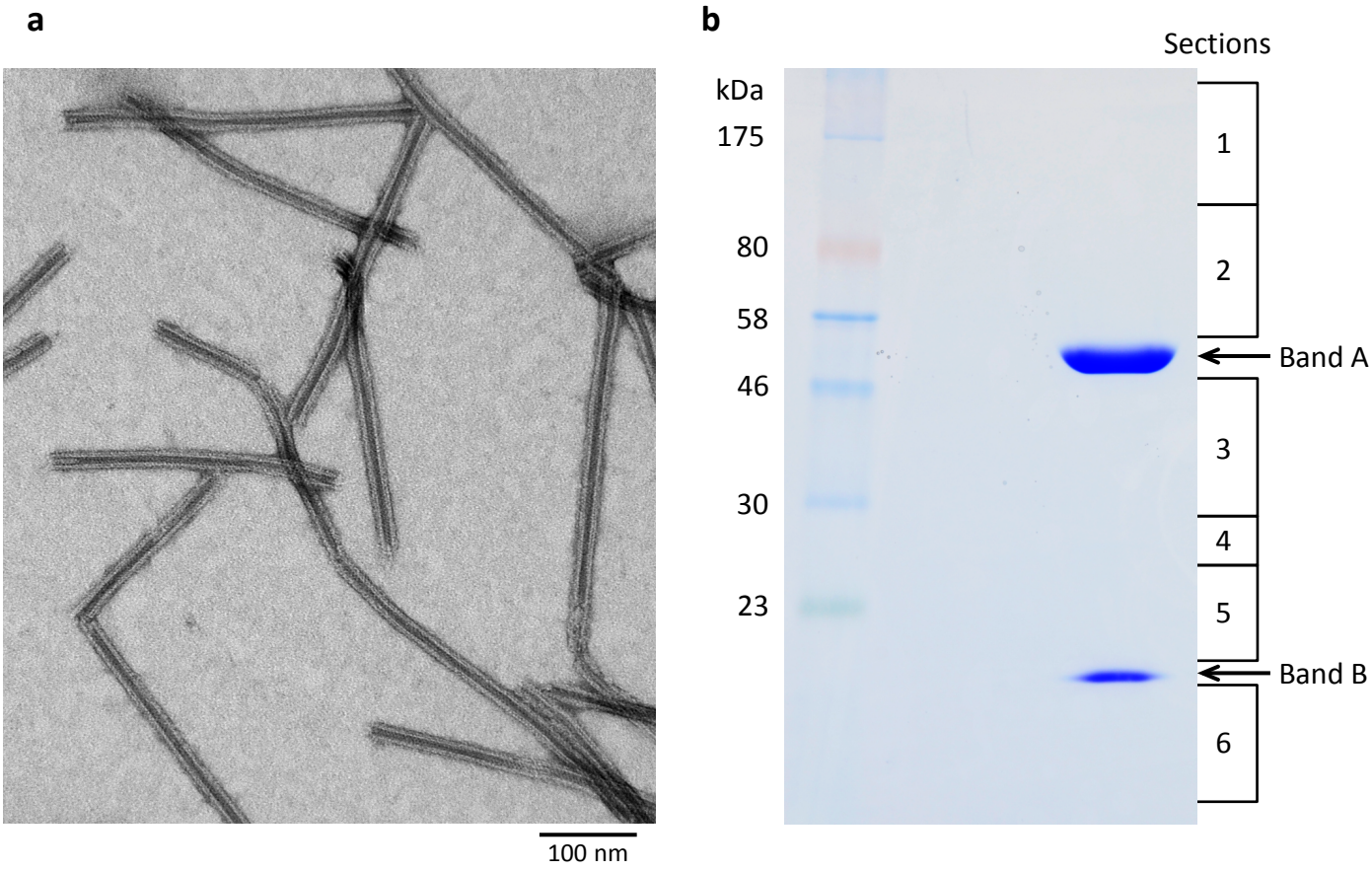

Supplementary Figure S9. Purified sheath - EM, SDS-PAGE analysis. Sheaths isolated from non-flagellated *V. cholerae* 2740-80 were purified from cytosolic proteins by three rounds of ultracentrifugation. **(a)** Sheath visualized by EM after uranyl formate negative staining. **(b)** A sample of the purified sheath (about 20 µg) was separated by 10-20% pre-cast polyacrylamide gel. The gel was stained by Coomassie blue R-250. After destaining two visible bands and 6 sections of the gel were cut out and protein content was determined by MS. Band A contained mostly VipB protein and Band B mostly VipA protein. Complete results from MS analysis are in **Supplementary Table 2**.

Supplementary Figure S10

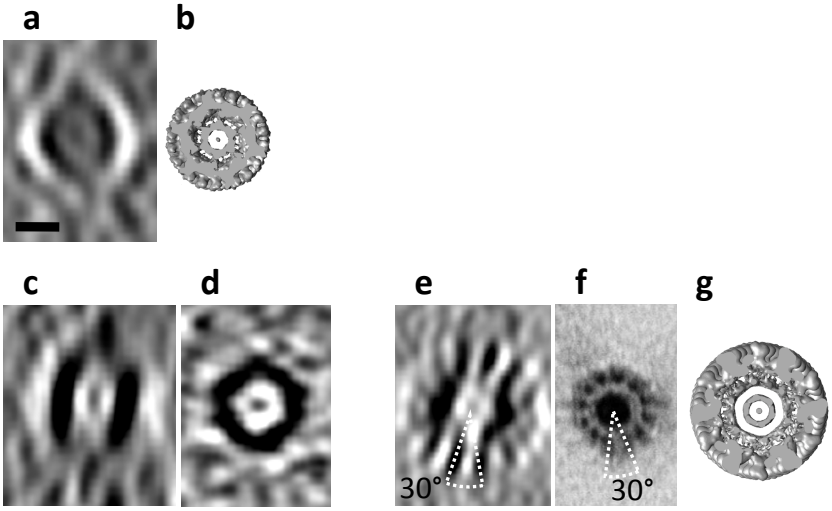

Supplementary Figure S10. Cross-sections through T6SS and phage sheaths. Top row: extended structures, **bottom row**: contracted structures. (**a, c, d**) 190-nm cryotomographic slices through T6SS sheaths within intact cells. (**e**) 19-nm cryotomographic slice through a purified T6SS sheath. (**f**) projection image of a negatively stained T6SS sheath (**b, g**) cross-sections through space-filling models of T4 phage sheath (created in Chimera from EMDB 1086 and 1126 maps). While panels a, c, and e are of sheaths that lay parallel to the sample grid, d is of a sheath that was oriented perpendicular. Because useful EM images cannot be obtained of samples tilted further than ~65˚, there is a "missing wedge" of data in reciprocal space that manifests as a blurring of the reconstruction perpendicular to the sample grid (the "z" direction). Thus tubular objects lying in the plane of the sample look like parentheses facing each other in slices perpendicular to the grid ("xz" slices), with the "top" and "bottom" of the ring missing (panels a, c, and e). Panel d therefore gives a superior view, since it is an "xy" slice without blur. In addition to the missing wedge, electron cryotomograms also suffer from the point-spread-function of the microscope, which like a low-pass-filter causes densities to appear as dark regions surrounded by bright fringes, or "halos". Thus in panels c and d it can be seen that contracted tubes are hollow, since they have bright interiors. Comparing panels c and a, however, reveals that extended tubes (panel a) are filled. This is also made clear in panel a itself through the difference in intensity immediate outside the tube (bright white) and the interior (medium grey). The medium grey interior is the superposition of density there with the white fringe from the sheath. Panel e has higher resolution and clarity (signal-to-noise-ratio) because it is of a purified sheath frozen in a very thin film of dilute buffer. As a result, the features within a much thinner slice (19-nm) are already clear, revealing the helical "paddles" that wrap around the sheath and are therefore averaged out in thicker slices (panels c and d). Panel e and f shows that the paddles are spaced every 30˚, corresponding to 12 around the circumference of the tube. Again because of the missing wedge effect, the central ring density is apparent on the sides (where its tangent is parallel to z), but the thin flat paddles appear best at the top and bottom (where their faces are parallel to z). The fact that there are 12 paddles around the T6SS (just as there are in contracted phage tails) is made even more clear in the negatively-stained sheath fragment imaged down its long axis (panel f). In negatively-stained images, the protein is light and the stain inside the tube and between the paddles is dark. Bar, 10 nm.

Supplementary Figure S11

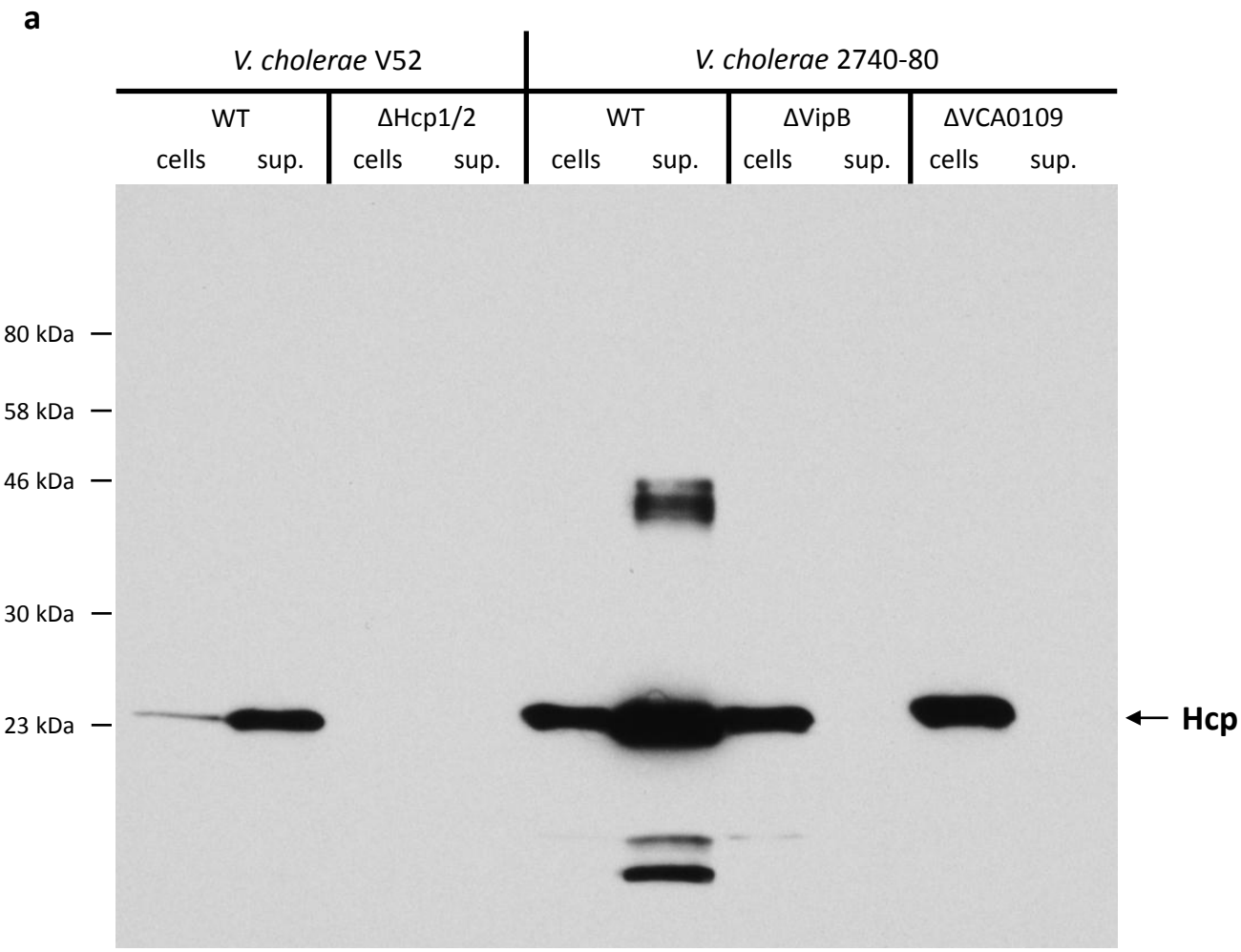

Supplementary Figure S11

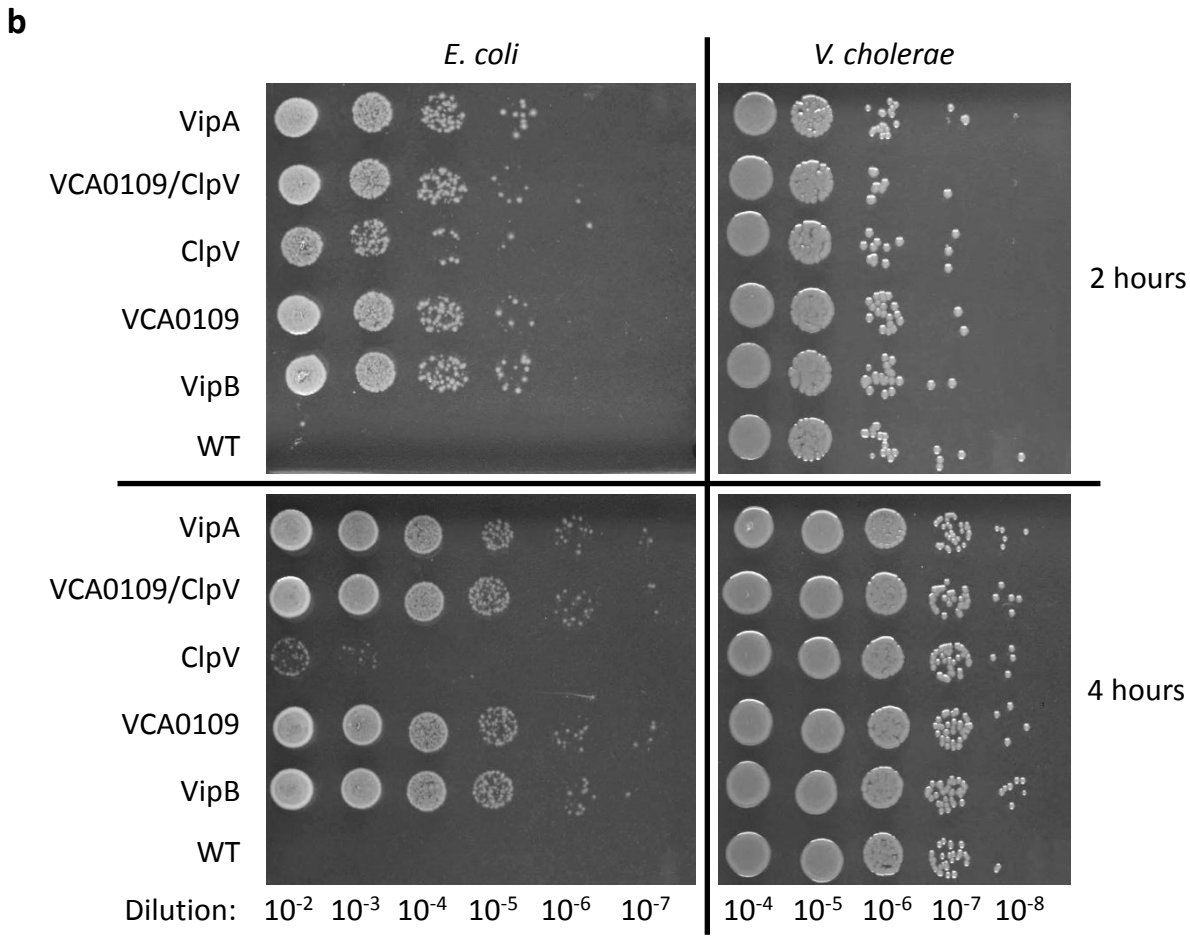

Supplementary Figure S11. **(a) Secretion of Hcp by T6SS.** Wild type strains V52 and 2740-80 as well as indicated mutants with both copies of Hcp genes, VipB or VCA109 genes deleted were grown as described in Methods and protein samples were prepared for western blot analysis. Hcp protein was detected in a cell lysate (cells) and a cell free supernatant (sup.) by western blot using anti-Hcp peptide specific antibody. Absence of the signal in V52 ΔHcp1/2 cells confirms specificity of the antibody. **(b) Quantification of *E. coli* killing by *V. cholerae*.** *E. coli* was mixed with *V. cholerae* in a ratio 1:10 and spotted on a LB plate. After 2 or 4 hours of incubation at 37 °C the cells were washed from the agar, serially diluted and spotted on a plate to select for *E. coli* or *V. cholerae*.

Supplementary Table 1. Abundance of T6SS structures observed by ECT in wild type cells.

no. of cells	no. of extended structures	no. of contracted structures
9	0	1
4	0	2
1	0	3
2	0	4
3	1	0
1	2	0
3	1	1
2	2	2
1	1	2
64	0	0

Note that slightly lower abundance compared to fluorescence microscopy is seen by ECT since in most cases only partial cells can be imaged.

Supplementary table 2 – MS analysis results

Sample[a]	Unique peptides[b]	Total peptides[c]	VC number[d]	Protein name[e]
Band A 55 kDa	**73**	**657**	**VCA0108**	**VipB**
	6	6	VC2412	dihydrolipoamide dehydrogenase
	5	5	VC1726	glycogen synthase
Band B 20 kDa	**28**	**384**	**VCA0107**	**VipA**
	19	**28**	**VCA0108**	**VipB**
	6	6	VC2579	30S ribosomal protein S5
	4	7	VC0360	30S ribosomal protein S7
	3	3	VC0570	50S ribosomal protein L13
Section 1 100-200 kDa	**36**	**86**	**VCA0108**	**VipB**
	39	43	VC0329	DNA-directed RNA polymerase subunit beta'
	25	27	VC0328	DNA-directed RNA polymerase subunit beta
	20	24	VC2030	ribonuclease E
	13	**19**	**VCA0107**	**VipA**
	7	7	VC1492	hypothetical protein
	5	5	VC2599	ribonuclease R
	3	3	VC2593	50S ribosomal protein L2
Section 2 55-100 kDa	**61**	**453**	**VCA0108**	**VipB**
	17	**50**	**VCA0107**	**VipA**
	20	34	VC2413	dihydrolipoamide acetyltransferase
	22	32	VC2664	chaperonin GroEL
	14	20	VC0855	molecular chaperone DnaK
	15	18	VC1866	formate acetyltransferase
	13	16	VC0251	acyl protein synthase/acyl-CoA reductase RfbN
	10	**10**	**VCA0116**	**ClpV**
	8	9	VC2342	elongation factor G
	7	7	VC2414	pyruvate dehydrogenase, E1 component
	6	6	VC2030	ribonuclease E
	5	5	VC2746	glutamine synthetase
	4	4	VC0723	polyphosphate kinase
	4	4	VC1920	ATP-dependent protease LA
	4	4	VC2430	DNA topoisomerase IV subunit A
	3	3	VC0643	translation initiation factor IF-2
Section 3 25-55 kDa	**45**	**177**	**VCA0108**	**VipB**
	20	46	VC2593	50S ribosomal protein L2
	15	**35**	**VCA0107**	**VipA**
	20	30	VC0321	elongation factor Tu

Sample[a]	Unique peptides[b]	Total peptides[c]	VC number[d]	Protein name[e]
	18	**29**	**VCA0114**	**hypothetical protein**
	11	18	274080_2667	major head subunit
	10	15	VC0349	hflK protein
	7	13	VC2397	cell division protein FtsZ
	10	12	VC0350	hflC protein
	11	11	VC2188	flagellin core protein A
	8	11	VC2183	ribose-phosphate pyrophosphokinase
	9	10	VCA0250	alpha-amylase
	9	10	274080_2763	type II secretory pathway protein
	5	9	VC2397	cell division protein FtsZ
	6	8	VC1179	pseudouridine synthase family 1 protein
	6	6	VC0856	dnaJ protein
	5	5	VC2086	dihydrolipoamide succinyltransferase
	5	5	VC0325	50S ribosomal protein L1
	4	5	VC0637	cell division protein FtsH
	4	4	VC2193	flagellar basal body P-ring protein
	3	3	VC2413	dihydrolipoamide acetyltransferase
	3	3	VC0250	iron-containing alcohol dehydrogenase, RfbM
	3	**3**	**VCA0111**	**hypothetical protein**
Section 4 ~25 kDa	**47**	**201**	**VCA0108**	**VipB**
	15	37	VC2590	30S ribosomal protein S3
	19	35	VC0325	50S ribosomal protein L1
	11	**18**	**VCA0107**	**VipA**
	5	6	VC0247	lipopolysaccharide/O-antigen transport protein
	5	5	VC2596	50S ribosomal protein L3
	4	4	VC2572	30S ribosomal protein S4
	4	4	VC0415	rod shape-determining protein MreB
	3	3	VC2593	50S ribosomal protein L2
Section 5 20-25 kDa	**39**	**88**	**VCA0108**	**VipB**
	18	**42**	**VCA0107**	**VipA**
	12	23	VC2595	50S ribosomal protein L4
	11	12	VC2590	30S ribosomal protein S3
	6	11	VC2572	30S ribosomal protein S4
	5	7	VCA0288	initiation factor IF3
	4	7	VC2593	50S ribosomal protein L2
	4	**4**	**VCA0114**	**hypothetical protein**
	4	4	VC0321	elongation factor Tu
	4	4	VC0152	DNA-binding transcriptional repressor FabR

Sample[a]	Unique peptides[b]	Total peptides[c]	VC number[d]	Protein name[e]
	4	4	VC2584	50S ribosomal protein L5
	3	3	VC2270	riboflavin synthase subunit alpha
	3	3	VC2581	50S ribosomal protein L6
Section 6 10-20 kDa	**21**	**145**	**VCA0107**	**VipA**
	29	**60**	**VCA0108**	**VipB**
	12	43	VC2586	50S ribosomal protein L14
	12	35	VC2597	30S ribosomal protein S10
	10	32	VC0369	50S ribosomal protein L9
	11	28	VC0564	50S ribosomal protein L19
	10	26	VC2591	50S ribosomal protein L22
	9	24	VC0435	50S ribosomal protein L21
	11	20	VC2570	50S ribosomal protein L17
	9	16	VC0324	50S ribosomal protein L11
	8	15	VC2574	30S ribosomal protein S13
	4	15	VC2573	30S ribosomal protein S11
	7	14	VC2580	50S ribosomal protein L18
	8	12	274080_A0464	hypothetical protein
	8	12	VC2577	50S ribosomal protein L15
	4	12	VC0218	50S ribosomal protein L28
	6	11	VC0366	30S ribosomal protein S6
	7	10	VC0571	30S ribosomal protein S9
	5	10	VC2583	30S ribosomal protein S14
	4	10	VC0520	30S ribosomal protein S21
	5	9	VC0359	30S ribosomal protein S12
	4	9	VC0436	50S ribosomal protein L27
	6	8	VC0326	50S ribosomal protein L10
	5	8	VC0368	30S ribosomal protein S18
	5	8	VCA0290	50S ribosomal protein L20
	4	8	VC2594	50S ribosomal protein L23
	5	6	VC0018	16 kDa heat shock protein A
	4	6	VC2578	50S ribosomal protein L30
	3	6	VC0679	30S ribosomal protein S20
	4	5	VC2585	50S ribosomal protein L24
	3	**5**	**VCA0109**	**gp25-like**
	3	5	VC0646	30S ribosomal protein S15
	3	3	VC0749	NifU family protein
	3	3	VC2593	50S ribosomal protein L2

[a] Sections or bands were cut from the SDS-PAGE gel and submitted separately for MS analysis. See Supplementary Figure 9b for gel.

[b] Number of unique peptides matching a particular *Vibrio* protein detected in the sample.

[c] Total number of peptides detected for a particular protein in the sample.

[d] Protein identification numbers.

[e] Protein name based on the latest available annotation.

T6SS related proteins are shown in bold.

SUPPLEMENTARY VIDEO LEGENDS

Supplementary Video 1. Time-lapse fluorescence microscopy of VipA-sfGFP dynamics, high magnification. VipA-sfGFP was expressed in ΔVipA background of *V. cholerae* 2740-80. 20 individual 10 minutes long time-lapse videos were obtained with a frame rate of 10 sec per frame. Video shows 3x3 μm region and plays 50x faster than real-time. It shows several extensions of VipA-sfGFP structures from one side of the cell to another followed by a contraction event and apparent disassembly of the contracted VipA-sfGFP structure. Time shown in the first 3 video segments corresponds to the timeline shown in Figure 1a. 4 min 4 s play time. MOV file, size 10 MB.

Supplementary Video 2. Time-lapse fluorescence microscopy of VipA-sfGFP dynamics. VipA-sfGFP was expressed in ΔVipA background of *V. cholerae* 2740-80. Two 10 minutes long time-lapse videos obtained with a frame rate of 10 sec per frame showing 48 x 36 μm field of cells. Video plays 50x faster than real-time. 24 s play time. MOV file, size 6.4 MB.

Supplementary Video 3. High speed time-lapse fluorescence microscopy of VipA-sfGFP contraction. VipA-sfGFP was expressed in ΔVipA background of *V. cholerae* 2740-80. Fluorescence of VipA-sfGFP was detected at speed of 8.5 frames per second (118 ms between frames, 50 ms exposure) in the first video segment, 50 frames per second (20 ms exposure time) in the segment number two, and 200 frames per second (5 ms exposure time) in the segments number 3, 4, and 5. All video segments show 30

frames before and after contraction. Gaussian blur filter (sigma radius = 1) was applied to individual frames of video in segments 2-5 to reduce noise and improve visual appearance without affecting time resolution. The field is about 3x3 μm. Video plays at speed of 10 frames per second. 31 s play time. MOV file, size 1.8 MB.

Supplementary Video 4. Time-lapse fluorescence microscopy of VipA-sfGFP dynamics at different expression levels of VipA-sfGFP in ∆VipA background. VipA-sfGFP was expressed in ∆VipA background of *V. cholerae* 2740-80 at four different induction levels. 5 minutes long time-lapse video (obtained with a frame rate of 10 sec per frame) showing 48 x 36 μm field of cells. Video plays 50x faster than real-time. Induction levels were 0.01% arabinose for segment 1, 0.003% for segment 2, 0.001% for segment 3, and 0.0003% for segment 4. 24 s play time. MOV file, size 6.2 MB.

Supplementary Video 5. Time-lapse fluorescence microscopy of VipA-sfGFP dynamics at different expression levels of VipA-sfGFP in wild-type background. VipA-sfGFP was expressed in wild-type background of *V. cholerae* 2740-80 at four different induction levels. 5 minutes long time-lapse video (obtained with a frame rate of 10 sec per frame) showing 48 x 36 μm field of cells. Video plays 50x faster than real-time. Induction levels were 0.01% arabinose for segment 1, 0.003% for segment 2, 0.001% for segment 3, and 0.0003% for segment 4. 24 s play time. MOV file, size 7.8 MB.

Supplementary Video 6. Time-lapse fluorescence microscopy of VipA-sfGFP dynamics in V52 strain. VipA-sfGFP was expressed in ΔVipA background of *V. cholerae* V52. 10 minutes long time-lapse video (obtained with a frame rate of 10 sec per frame) showing 48 x 36 μm field of cells. Video plays 50x faster than real-time. 12 s play time. MOV file, size 2.7 MB.

Supplementary Video 7. Time-lapse fluorescence microscopy of VipA-mCherry2 dynamics. VipA-mCherry2 was expressed in ΔVipA background of *V. cholerae* 2740-80. 5 minutes long time-lapse video (obtained with a frame rate of 10 sec per frame) showing 48 x 36 μm field of cells. Video plays 50x faster than real-time. 6 s play time. MOV file, size 2.1 MB.

Supplementary Video 8. Time-lapse fluorescence microscopy of VipA-sfGFP in Δ ClpV background. VipA-sfGFP was expressed in ΔVipA/ΔClpV background of *V. cholerae* 2740-80. Two 5 minutes long time-lapse video (obtained with a frame rate of 6 sec per frame) showing 48 x 36 μm field of cells. Video plays 30x faster than real-time. 20 s play time. MOV file, size 5.3 MB.

Supplementary Video 9. Time-lapse fluorescence microscopy of VipA-sfGFP in ΔVCA0109 background. VipA-sfGFP was expressed in ΔVipA/ΔVCA0109 background of *V. cholerae* 2740-80. Two 5 minutes long time-lapse videos (obtained with a frame rate of 6 sec per frame) showing 48 x 36 μm field of cells. Video plays 30x faster than real-time. 20 s play time. MOV file, size 5.4 MB.

Supplementary Video 10. 3-D tomographic analysis showing that a T6SS tubular structures are clearly located in the cytoplasm. The movie starts moving up and down through 2D tomographic slices of the wild type cell shown in **Figure 2e**. Later, 3D segmentations of contracted T6SS (red), baseplate (yellow), inner membrane (blue) and outer membrane are shown. 40 s play time. MOV file, size 29.3 MB.

Supplementary Video 11. The bacterial T6SS is a spring-loaded poison dagger. The movie shows the main results of fLM and cryo-EM imaging. It further includes an animation of the proposed T6S mechanism shown in Fig. 4. The movie has a narration. 2 min 23 s play time, MOV file, size 27.6 MB.